CHIN. PHYS. LETT. Vol. 34, No. 3 (2017) 034701

# Determination of Slip Length in Couette Flow Based on an Analytical Simulation Incorporating Surface Interaction *

Xin Zhao(赵欣), Chao Wei(魏超)**, Shi-Hua Yuan(苑士华)

*Science and Technology on Vehicle Transmission Laboratory, Beijing Institute of Technology, Beijing 100081*

(Received 12 September 2016)

*An analytical simulation based on a new model incorporating surface interaction is conducted to study the slip phenomenon in the Couette flow at different scales. The velocity profile is calculated by taking account of the micro-force between molecules and macro-force from the viscous shearing effect, as they contribute to the achievement of the slip length. The calculated results are compared with those obtained from the molecular dynamics simulation, showing an excellent agreement. Further, the effect of the shear rate on the slip is investigated. The results can well predict the fluid flow behaviors on a solid substrate, but has to be proved by experiment.*

*PACS:* 47.10.A−, 47.15.St, 47.61.Fg, 47.85.ld DOI: 10.1088/0256-307X/34/3/034701

The 'no-slip' boundary condition, i.e., zero flow velocity at a wall, has been applied in the calculation of fluid flow from continuum hydrodynamics theory for a long time,[1] and some experimental evidence does support this assumption at macroscopic scales.[2] However, the difference between the simulation based on no-slip assumption and experiment becomes pronounced when the scale of interest goes down to microns or below.[3,4] According to the micro-flow experiment, Vinogradova[4] found that the real hydrodynamic pressure is different from the simulation values based on no-slip assumption, and finally she modified her model by applying the slip boundary condition and successfully explained the experimental results. In fact, slip has been proved to exert a significant effect on the flow properties in microfluidic devices prepared for biomaterials synthesis[5,6] as well as medical diagnostics,[7] and engineering, for example, the oil film pressure and dynamic characteristics of journal bearing in the conventional lubricant system were affected by slip.[8,9] Therefore, the effect of slip triggers significant attention.[10,11]

Slip frequently occurs at various scales, and the effect becomes prominent at microscale. The mechanism of slip has been researched widely by both experimental and theoretical ways. Experimental methods can be divided into direct and indirect methods. The direct methods such as u-PIV[12] and FCS[13,14] are capable of observation of the slip phenomenon through the analysis of image from fluorescence particles close to the wall. The indirect method is carried out by comparing the measured results of the variation in the liquid flow rate[15] and force from the surface force apparatus[16,17] or atomic force microscopy[18] with a theory prediction under the no-slip boundary condition. Further, the slip length as an important parameter to describe the slip level can be derived from the measurement results according to a modified model taking the slip into account. However, an essential shortage in direct and indirect methods is the less resolution in the determination of the velocity close to the wall and slip length.

In the aspect of theoretical investigation, a linear-slip-length model was first proposed by Navier *et al.*[19] in 1823, assuming the slip level as constant under different conditions. Obviously, the assumption is easy to use, but its correction still needs improvement. With the development of the molecular dynamic simulation, a more accurate trend of the slip length varying with the shear rate is achieved, exhibiting a non-linear relationship.[20,21] The molecular dynamics (MD) method has won the favor of researchers, as it can recur the slip phenomenon at molecular scale. However, with the scale of the system increasing from several nanometers[22] to hundreds of namometers,[23] it is too slow to simulate the behavior of fluid with respect to a large amount of particles. Thus the MD simulation is mainly used in the scale less than micrometers. Moreover, the MD model has many quantum parameters, which are not easy to determine and thus affect the simulation precision.

In this study, a new analytical velocity slip model was developed to investigate the slip phenomenon in the Couette flow at different scales. Different from the traditional MD model, this model takes both micro force and macro force into account and uses less quantum parameters than those in the MD model to obtain the distributions of fluid density and velocity in the region close to the wall. Further, this method can perform slip in the case with gap height larger than nanometers in a more efficient way, where the continuum theory still can be used.[24,25] The simulation and MD results were proposed, and a good agreement was achieved. The effect of the shear rate on the slip was investigated, indicating good prediction of the fluid flow behaviors on a solid substrate but yet to be con-

*Supported by the National Natural Science Foundation of China under Grant No 51305033, and the Ministry of National Defense of China under Grant No 9140C340506.

**Corresponding author. Email: pekingbit@163.com

© 2017 Chinese Physical Society and IOP Publishing Ltd

firmed by experiments.[26,27]

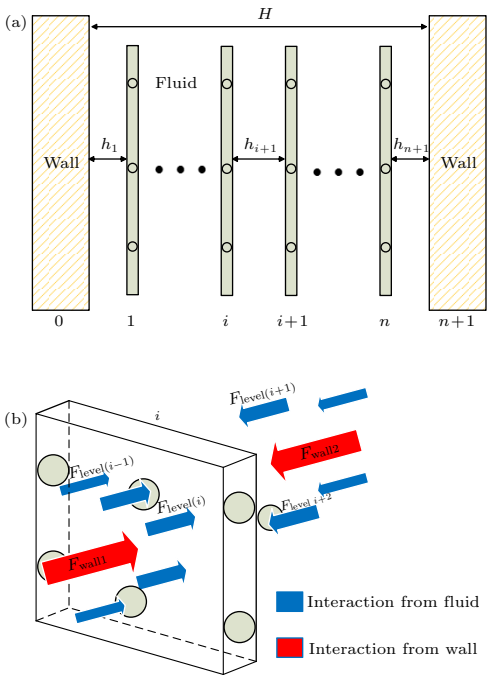


**Fig. 1.** (a) Schematic illustration of force analysis of the micro fluid layer (MFL) model in the thickness direction. (b) The force schematic of the $i$th layer in the thickness direction.

Figure 1(a) shows the schematic illustration of the MLF Model. The inside fluid is trapped in two movable walls. The distance between the two walls is set as $H$, and the inside fluid is divided into $(n+1)$ layers in the thickness direction. Note that one wall is named as the 0th layer, the other wall is named as the $(n+1)$th layer, and distance between the $i$th and the $(i+1)$th layer is named as $h_{i+1}$. The total number of molecules, $N$, in each layer is assumed to be equal and tends to infinity, and as a result the fluid layer can be seen as an infinite plane for a molecule. All the molecules in a layer are assumed to have the same distance from the wall or the adjacent layer, and therefore they own the same forcing state. Figure 1(b) shows the force schematic of the $i$th layer in the thickness direction. For the $i$th layer, it suffers forces from the wall and the adjacent fluid layers, and the force equilibrium equation can be expressed as

$$\sum_{j=1}^{2} F_{\mathrm{w},j} + \sum_{k=1,k\neq i}^{n} F_{\mathrm{l},k} = 0, \tag{1}$$

where $F_{\mathrm{w},j}$ is the force exerting on the $i$th layer from the wall, $j=1$ and 2 represent the force from one and other wall, respectively, and $F_{\mathrm{l},k}$ represents the force from the $k$th fluid layer.

For a certain layer, $F_{\mathrm{w},j}$ and $F_{\mathrm{l},k}$ are equal to the sum of the force acting on a molecule in this layer from the wall and fluid layers, respectively. According to the assumption that the forcing state of all the molecules in a layer remains the same, Eq. (1) can be transformed to

$$N \times \left( \sum_{j=1}^{2} F^{\mathrm{s}}_{\mathrm{w},j} + \sum_{k=1,k\neq i}^{n} F^{\mathrm{s}}_{\mathrm{l},k} \right) = 0, \tag{2}$$

where $F^{\mathrm{s}}_{w,j}$ and $F^{\mathrm{s}}_{\mathrm{l},k}$ represent the forces acting on a single molecule from the $j$th wall and the $k$th layer, respectively. Obviously, the solution of Eq. (2) is based on the determination of parameters $n$, $F^{\mathrm{s}}_{w,j}$ and $F^{\mathrm{s}}_{\mathrm{l},k}$.

The total number of layer $n$ can be calculated by $n = H/\sigma$, where $\sigma$ is the average distance between the two adjacent layers. As the total molecular quantity of each layer remains unchanged, $\sigma$ is determined by

$$\sigma = \sigma_0 \frac{\rho_0}{\rho(p)}, \tag{3}$$

where $\sigma_0$ and $\rho_0$ represent the distance parameters of the potential function and the fluid density under the condition of ambient pressure, respectively, and $\rho(p)$ represents the density under the conditions of working pressure.

For forces $F^{\mathrm{s}}_{w,j}$ and $F^{\mathrm{s}}_{\mathrm{l},k}$ acting on a single molecule, these two forces exert on a single molecule from an infinite wall surface and the $k$th layer, respectively. They can be deduced by the L–J potential function represented by

$$\begin{aligned} F^{\mathrm{s}}_{\mathrm{w},j}(r_0) &= \frac{\partial \int_{r_0}^{\infty} U(r)dr}{\partial r_0} \\ &= 2\pi\rho_{\mathrm{w}} \left[ -2\varepsilon_{\mathrm{w}}(\sigma_{\mathrm{w}})^9 \frac{1}{r_0^8} + 3\varepsilon_{\mathrm{w}}(\sigma_{\mathrm{w}})^6 \frac{1}{r_0^5} \right], \end{aligned} \tag{4}$$

$$\begin{aligned} F^{\mathrm{s}}_{\mathrm{l},k}(r_1) &= \frac{\partial \int_{r_0}^{\infty} U(r)dr}{\partial r_1} \\ &= 2\pi\rho_{\mathrm{f}} \left[ -2\varepsilon_{\mathrm{f}}(\sigma_{\mathrm{f}})^9 \frac{1}{r_1^8} + 3\varepsilon_{\mathrm{f}}(\sigma_{\mathrm{f}})^6 \frac{1}{r_1^5} \right], \end{aligned} \tag{5}$$

where $\sigma_{\mathrm{w}}$ and $\varepsilon_{\mathrm{w}}$ are the distance and energy parameters of the wall, respectively, and $\sigma_{\mathrm{f}}$ and $\varepsilon_{\mathrm{f}}$ are those of the fluid, $r_0\,(r_1)$ represent the distance between the molecule and wall (the $k$th fluid layer), and $\rho_{\mathrm{w}}$ is the density of the wall. For the molecular number of the fluid layer, $\rho_{\mathrm{f}}$ is obtained by the following equation $\rho_{\mathrm{f}} = \rho_{\mathrm{f}(p)}(\sigma_{\mathrm{f}}/d_0)$ as the total amount of fluid molecules remains the same, with $d_0$ being the average distance between the two adjacent molecules and can be deduced from the density relationship. Assuming $M$ as the number of fluid molecules and $V$ as the volume occupied by these molecules, and assuming that these molecules distribute uniformly and the volume of each molecule is $kd_0^3$, where $k$ is the volume parameter, the relationship between $V$ and $d_0$ is expressed by $V = kd_0^3$. Further, assuming $m_{\mathrm{e}}$ as the mass of a single molecule, the mass density of fluid can be obtained by $\rho_{\mathrm{f}} = Mm_{\mathrm{e}}/Mkd_0^3$. According to this equation, the average distance between the two adjacent molecules can be obtained by $d_0 = (m_{\mathrm{e}}/k\rho_{\mathrm{f}})^{1/3}$. It is of particular concern that the energy parameter of the wall $\varepsilon_{\mathrm{w}}$ reflects the acting effects of the wall on the fluid

layer. Increasing $\varepsilon_{\rm w}$ can increase the sticking force of the wall on the fluid layer close to the surface, as contributes to the formation of adhesive layer.

The interacting force between two molecules decreases sharply with increasing the distance. Especially when the distance is larger than $3\sigma_0$ ($3\sigma_0$ is called the cutoff radius), the interacting force can be ignored.[28] Therefore, to simplify the solution, the effect of cutoff radius is taken into account in the calculation of the force acting on a single fluid molecule from an infinite surface. Here $\sigma_0 \approx \sigma$. Consequently, for the $i$th layer, Eq. (2) can be simplified to

$$N \times \Big( \sum_{j=1}^{2} F^{\rm s}_{{\rm w},j}(h_1, \ldots, h_{n+1}) + \sum_{k=-3,k\neq 0}^{3} F^{\rm s}_{{\rm l},i+k}(h_1, \ldots, h_{n+1}) \Big) = 0. \quad (6)$$

To solve these equations, a new equation is added as $\sum_{i=1}^{n+1} h_i = H$.

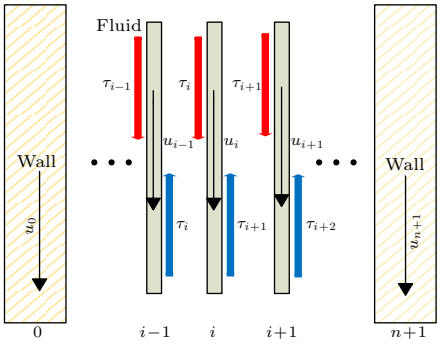


**Fig. 2.** Schematic illustration of force analysis of the MFL model in the shear direction. Here $u_i$ represents the velocity in the $i$th layer.

The force analysis in the shear direction is shown in Fig. 2. We assume that $v_1$ and $v_2$ are the shear velocities of two walls. When the wall moves, the fluid layer suffers from the shearing forces from the adjacent layers on both sides, and these shearing forces are equal due to the force equilibrium in the shear direction. According to the experimental results of the confined fluid obtained from SFA,[25] the continuum theory can be used in several nanometers. Thus in the MFL model, the shear stress $\tau_i$ is expressed by $\eta_i du_i/dh_i$. As the distance between two adjacent layers is very small, $du_i/dh_i$ can be replaced by $(u_i - u_{i-1})/dh_i$. Due to this, the shearing force equilibrium relationship is expressed as

$$\tau_n = \tau_{n+1} \Rightarrow \frac{\eta_i}{h_i}(u_i - u_{i-1}) = \frac{\eta_{i+1}}{h_{i+1}}(u_{i+1} - u_i), \quad (7)$$

where $u_1$, $u_2$, …, $u_i$,…, $u_n$ represent the velocities of the fluid layer and $\eta_1$, $\eta_2$,…, $\eta_i$,…, $\eta_n$ represent the viscosities of the fluid layer. To calculate the viscosity of the fluid layer, a new parameter 'layer density' is defined, representing the ratio of the fluid mass to the volume established by the adjacent layers. The fluid mass between the $(i-1)$th layer and the $i$th layer, $M_{{\rm spacei}}$, is equal to the sum of half the masses of the adjacent layers by $M_{{\rm spacei}} = 0.5(M_{i-1} + M_i)$, where $M_{i-1}$ and $M_i$ represent the mass of the molecules in the $(i-1)$th and $i$th layer, respectively. Therefore, the layer density is expressed by $\rho_i = 0.5(M_{i-1} + M_i)/(Ah_i)$, where $A$ is the cross-sectional area of the fluid layer. Particularly, for the first and last layers, as the wall has no contribution to the fluid mass, the layer density is expressed by $\rho_i = 0.5M_i/(Ah_i)$, $(i = 1,\ n+1)$. Finally, the relationships between the ratio of the layer density are obtained by

$$\begin{aligned} \frac{\rho_1}{\rho_2} &= \frac{h_2}{2h_1}, \\ &\ldots, \\ \frac{\rho_i}{\rho_{i+1}} &= \frac{h_{i+1}}{h_i}, \\ &\ldots, \\ \frac{\rho_n}{\rho_{n+1}} &= \frac{2h_{n+1}}{h_n}. \end{aligned} \quad (8)$$

Note that the working parameters such as pressure and temperature are close to the central layer and are equal to those under the ambient condition. Therefore, the value of $\rho_{n/2}$ is equal to $\rho_{\rm f}$, and the layer densities $\rho_1$, $\rho_2$,…, $\rho_i$,…, $\rho_n$ and $\rho_{n+1}$ can be deduced, correspondingly. Based on the obtained layer density, the layer viscosities $\eta_1$, $\eta_2$,…, $\eta_i$,…, $\eta_n$ are easy to calculate according to the relationship between the density and viscosity.[29,30] As a result, the values of $u_1$, $u_2$,…, $u_i$,…, $u_n$ can be obtained.

To prove the validation of the MFL model, a validation analysis is conducted in the case of hexadecane fluid and Fe wall, and compared with the MD results.[31,32] The physical properties are given as follows: $\sigma_{\rm Fe} = 0.3471\,{\rm nm}$, $\varepsilon_{\rm Fe} = 2.7718 \times 10^{-21}\,{\rm J}$, $\rho_{\rm w} = 7.9\,{\rm g/cm^3}$, $\sigma_{\rm H} = 0.4045\,{\rm nm}$, $\varepsilon_{\rm H} = 6.9722 \times 10^{-22}\,{\rm J}$, $\rho_0 = 0.7734\,{\rm g/cm^3}$, and $\eta_0 = 0.00034\,{\rm Pa{\cdot}s}$. Other parameters are listed in Table 1.

**Table 1.** Simulation parameters.

| Variables | Parameters | Simulation values |
|---|---|---|
| $H$ | Distance between two walls | $21\sigma$ |
| $p$ (GPa) | Pressure | 1.56 |
| $T$ (K) | Temperature | 300 |
| $v_1$ (m/s) | Velocity of 0th wall | 0 |
| $v_2$ (m/s) | Velocity of $(n+1)$th wall | 5 |
| $k$ | Volume parameter | 1 |
| $n$ | Total number of layer | 21 |

Figure 3(a) shows the variation in the fluid density with the distance from the wall for the new MFL model and the MD model. In general, the fluid density increases first, then decreases, and finally tends to be stable with increasing the distance to the wall by the two models. The tendency of the MFL model is in good agreement with the MD model. Figure 3(b) presents the variation in the slip velocity of the fluid

layer with the distance from wall for the two models. In the region close to the wall, there exists a large change in the density as shown in Fig. 3(a) for the cases of MDs and MFL ($\varepsilon_{\rm Fe} = 2.7718 \times 10^{-21}$ J), resulting in the same large change in viscosity. Therefore, a sharp change in the velocity occurs in this region, as shown in Fig. 3(b). For the MFL and MD models, the slip velocity shows the same changing tendency. The velocity changes sharply first, then remains unchanged in a small region, and finally varies steadily. The sharp velocity change in the region close to the wall proves the existence of boundary slip. However, in some special cases that the energy parameter $\varepsilon_{\rm w}$ is large enough to form the adhesive layer, the velocity change occurs on the adhesive layer while not on the wall surface, as results in the negative velocity slip length show in Fig. 3(b) for the case of $\varepsilon_{\rm w} = 4.7718 \times 10^{-21}$ J. This negative slip has been confirmed by experiment.[33,34]

Although the simulating results of our model show a good agreement with that of the MD model, there still exists a slight difference in the density and velocity in the region close to the wall. For the density, the peak density of our model is smaller than that in the MD model because the fluid density in our model is a local average of one layer. Therefore, the velocity changing rate in the region close to the wall for the MFL model is correspondingly smaller than that for the MD model. Meanwhile, in the case that the adhesive layer occurs, the fluid density close to the wall is larger than that without the adhesive layer, further the fluid density is close to that in the middle region, as shown in Fig. 3(a) for the case of $\varepsilon_{\rm w} = 4.7718 \times 10^{-21}$ J.

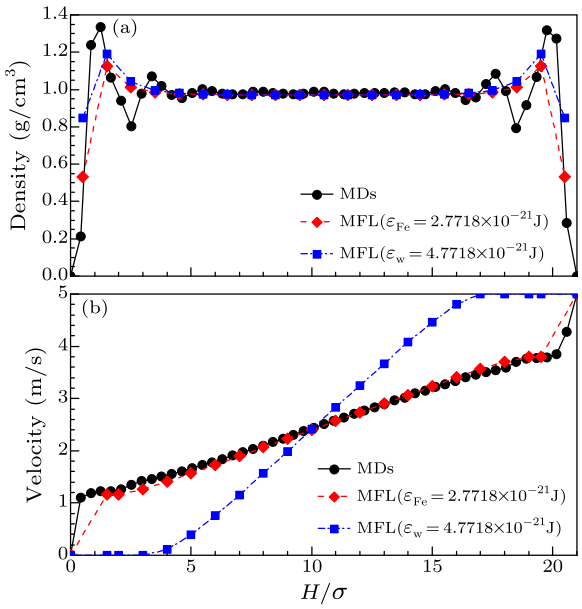


**Fig. 3.** (a) Distribution of fluid density for the MFL and MD models. The circle represents the results of the MD model. The diamond represents the results of MFL with $n = 21$. (b) Distribution of the fluid velocity by MFL and MD models.

According to the preceding analysis, the MFL model can simulate the slip characteristic similar to the MD model, but in less time. To investigate the effect of the shear rate on the slip, some simulations with different film thicknesses in the range of $21\sigma$–$13000\sigma$ are conducted by the MFL model. Except the thickness parameter, the other simulation parameters are the same as those shown in Fig. 3. Figure 4 shows the relationship between the slip length $b$ and the film thickness $H$. The slip length decreases sharply with the increasing film thickness. However, when the film thickness is larger than a critical level (here the critical level is close to $2000\sigma$), the slip length tends to be unchanged. When the velocity of the wall remains constant, the decrease in the film thickness will increase the shear rate, and in turn the increase of the slip length. Moreover, the relationship between the slip length and shear rate predicts well the fluid flow behaviors on a solid substrate and is yet to be confirmed by experiment.[26,27] However, in Ref. [26] since the critical value of the shear rate is smaller than that of ours, it is highly possible that the quantum parameters in our model are still inaccurate. Therefore, the discrepancies between the experimental and our model can be reduced if a more accurate parameter value can be obtained.

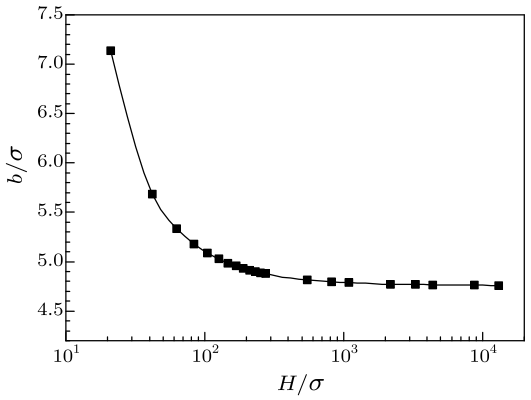


**Fig. 4.** Slip length varying with the film thickness.

In summary, the velocity profile confined in two walls can be calculated by a new developed velocity slip model. This model takes both micro force and macro force into account and uses less quantum parameters than those in the MD model to obtain the distributions of the fluid density and velocity in the region close to the wall. To verify the validation of this model, the density and velocity distribution between our model and the MD model are compared, and the results present a good agreement. Furthermore, the effect of the shear rate on the slip is investigated. The result shows that the slip length first decreases sharply with decreasing the shear rate (corresponding to an increase of the film thickness), and when the shear rate is less than a critical level, the slip length remains stable. This trend predicts well the fluid flow behavior by experiment. We believe that this method

contributes a novel and more efficient way to explore the phenomenon and characteristics of boundary slip. In addition, an intensive understanding of the mechanism of flow has important implications on the design of microfluidic devices and journal bearing.

## References


[1] Bernoulli D 1968 *Specimen Theoriae Novae de Mensura Sortis* (Paris: Gregg)
[2] Koplik J and Banavar J R 1995 *Annu. Rev. Fluid. Mech.* **27** 257
[3] Squires T M and Quake S R 2005 *Rev. Mod. Phys.* **77** 977
[4] Vinogradova O I 1995 *Langmuir* **11** 2213
[5] Beebe D J, Mensing G A and Walker G M 2002 *Annu. Rev. Biomed. Eng.* **4** 261
[6] Voldman J, Gray M L and Schmidt M A 1999 *Annu. Rev. Biomed. Eng.* **1** 401
[7] Valencia P M, Farokhzad O C, Karnik R and Langer R 2012 *Nat. Nanotechnol.* **7** 623
[8] Cheng F and Ji W X 2016 *Tribo. Int.* **97** 163
[9] Patel J R and Deheri G M 2016 *J. Appl. Fluid Mech.* **9** 855
[10] Bhattacharyya K, Mukhopadhyay S and Layek G C 2011 *Chin. Phys. Lett.* **28** 094702
[11] Chen Y Y, Yi H H and Li H B 2008 *Chin. Phys. Lett.* **25** 184
[12] Pierre J and Patrick T 2005 *Phys. Rev.* E **71** 035303
[13] Vinogradova O I, Koynov K, Best A and Feuillebois F 2009 *Phys. Rev. Lett.* **102** 118302
[14] Schaeffel D, Koynov K, Vollmer D, Butt H J and Schoenecker C 2016 *Phys. Rev. Lett.* **116** 134501
[15] Choi C H, Westin K J A and Breuer K S 2003 *Phys. Fluids* **15** 2897
[16] Baudry J, Charlaix E, Tonck A and Mazuyer D 2001 *Langmuir* **17** 5232
[17] Cottin-Bizonne C, Cross B, Steinberger A and Charlaix E 2005 *Phys. Rev. Lett.* **94** 056102
[18] Vinogradova O I and Yakubov G E 2006 *Phys. Rev.* E **73** 045302
[19] Navier C 1823 *France* **6** 389
[20] Thompson P A and Troian S M 1997 *Nature* **389** 360
[21] Martini A, Hsu H Y, Patankar N A and Lichter S 2008 *Phys. Rev. Lett.* **100** 206001
[22] Zhang H, Zhang Z and Ye H 2012 *Microfluid. Nanofluid.* **12** 107
[23] Cao B Y, Chen M and Guo Z Y 2005 *Appl. Phys. Lett.* **86** 091905
[24] Cui H H et al 2004 *Phys. Fluids* **16** 1803
[25] Bocquet L and Charlaix E 2010 *Chem. Soc. Rev.* **39** 1073
[26] Neto C, Craig V S J and Williams D R M 2003 *Eur. Phys. J.* E **12** 71
[27] Zhu Y and Granick S 2002 *Langmuir* **18** 10058
[28] Cieplak M, Koplik J and Banavar J R 2001 *Phys. Rev. Lett.* **86** 803
[29] Dowson D and Higginson G R 2014 *Elasto-Hydrodynamic Lubrication: International Series on Materials Science and Technology* (Guildford: Pergamon)
Bair S Winer W O 1992 *J. Tribol.* **114** 1
[30] Belonoshko A B, Ahuja R and Johansson B 2000 *Phys. Rev. Lett.* **84** 3638
[31] Jabbarzadeh A, Atkinson J D and Tanner R I 1999 *J. Chem. Phys.* **110** 2612
[32] Gruener S, Wallacher D, Greulich S, Busch M and Huber P 2016 *Phys. Rev.* E **93** 013102
[33] Gruener S and Huber P 2009 *Phys. Rev. Lett.* **103** 174501